

Pair-breaking effects and coherence peak in the terahertz conductivity of superconducting $\text{BaFe}_{2-2x}\text{Co}_{2x}\text{As}_2$ thin films

R. Valdés Aguilar,^{1,*} L. S. Bilbro,¹ S. Lee,² C. W. Bark,² J. Jiang,³ J. D. Weiss,³ E. E. Hellstrom,³ D. C. Larbalestier,³ C. B. Eom,² and N. P. Armitage^{1,†}

¹*The Institute of Quantum Matter, Department of Physics and Astronomy, The Johns Hopkins University, Baltimore, Maryland 21218, USA*

²*Department of Material Science and Engineering, University of Wisconsin, Madison, Wisconsin 53706, USA*

³*National High Magnetic Field Laboratory, Florida State University, Tallahassee, Florida 32310, USA*

(Received 21 July 2010; revised manuscript received 13 October 2010; published 19 November 2010)

We report a study of high quality pnictide superconductor $\text{BaFe}_{1.84}\text{Co}_{0.16}\text{As}_2$ epitaxial thin films using time-domain terahertz (THz) spectroscopy. Near T_c we find evidence for a coherence peak and qualitative agreement with the weak-coupling Mattis-Bardeen form of the conductivity. The real part of the THz conductivity is found to be not fully suppressed at low temperature and σ_2 is significantly smaller than the Mattis-Bardeen expectation. The temperature dependence of the penetration depth λ follows a power law with an unusually high exponent of 3.1. We interpret these results as consistent with impurity scattering-induced pair breaking. Taken together our results are strong evidence for an extended $s\pm$ order-parameter symmetry.

DOI: [10.1103/PhysRevB.82.180514](https://doi.org/10.1103/PhysRevB.82.180514)

PACS number(s): 74.70.Xa, 74.25.Gz, 74.78.-w

The discovery of iron-based superconductors (SCs) (Refs. 1–5) has further increased interest in the physics of high-temperature superconductivity. Among other things, this has stemmed from similarities in the phase diagram between high- T_c cuprates and these new superconductors. Both share a proximity and interplay with a magnetically ordered state, a superconducting dome as a function of doping and anomalous *normal-state* properties.^{6,7} However, significant differences also exist. For instance, for the iron-based materials the undoped parent compounds are metallic while the cuprates are Mott insulators. Also, in the cuprates, a single band model has been considered a good starting point to describe the basic physical picture, whereas the iron pnictides have multiple occupied d orbitals which make even a simple tight-binding model more involved.⁸

Based on local-density approximation first-principles calculations,⁹ it was suggested that a natural symmetry for the order parameter had a wave function with opposite signs for different sheets of the Fermi surface (FS), so-called extended s wave or $s\pm$ symmetry. This was based on the predicted band structure with two almost circular electron and hole pockets separated by the wave vector (π, π) , which matches the ordering magnetic wave vector in the undoped materials. This Fermi-surface geometry lends itself to a pairing scenario based on spin-wave exchange with that wave vector. An analysis based on a renormalization-group treatment gives a similar picture.¹⁰

One of the hallmarks of the BCS theory of ordinary superconductors¹¹ was the prediction of an energy gap to single-particle excitations. The theory was extended by Mattis *et al.*¹² to calculate the electrical conductivity as a function of temperature and frequency. They predicted that just below T_c , for frequencies below the gap 2Δ , the real part of the conductivity has an enhancement from “coherence factor” effects. These originate from the interference between the transition amplitudes of the electromagnetic field operator A between single-particle states. This occurs because the superconducting ground state is a *coherent* superposition of

single-particle states¹³ which participate in the scattering and absorption of the field.

In general, a coherence peak can arise when the portions of Fermi surface that are coupled by an experimental probe have gaps of the same sign and magnitude. The first evidence for it was in the NMR relaxation rate of Al.¹⁴ In the ac conductivity, the first observation of this effect was in Tinkham’s far-infrared-absorption experiments of lead.¹⁵ In the case of the iron-based superconductors, the coherence or Hebel-Slichter peak has not been observed in NMR experiments.^{16,17} Because NMR is a local probe and can couple parts of the FS that differ by large momentum transfer, the absence of the coherence peak has been interpreted as supporting the picture of the sign changing extended s -wave symmetry of the gap function ($s\pm$).^{9,10,18}

In this Rapid Communication we report evidence for the coherence peak in the terahertz (THz) conductivity of the iron pnictide $\text{BaFe}_{1.84}\text{Co}_{0.16}\text{As}_2$. Our results point to the existence of an order parameter that is more or less uniform over a FS sheet. We also find evidence for pair-breaking effects in the form of a residual real part of the conductivity at low temperature and a reduced superfluid density over the expected value. Together these results are consistent with an $s\pm$ symmetry of the order parameter which has opposite sign gaps on different FS sheets.

Thin films of $\text{BaFe}_{2-2x}\text{Co}_{2x}\text{As}_2$ were grown by pulsed laser deposition on $(\text{La,Sr})(\text{Al,Ta})\text{O}_3$ (LSAT) substrates with a SrTiO_3 (STO) template to allow epitaxial growth. Extensive details on the film growth and characterization can be found elsewhere.¹⁹ The novel template engineering results in films of exceptional quality. As shown in the inset to Fig. 1 the full width at half maximum of the (004) reflection rocking curve of the film on STO/LSAT is as narrow as 0.3° , which is the narrowest ever reported for 122 thin films whereas that of the film on bare LSAT is as broad as 4.1° . The small mosaic spread is comparable to good single crystals. Residual resistivity values (Fig. 1) of films grown on STO/LSAT are almost a factor of 2 smaller than those grown

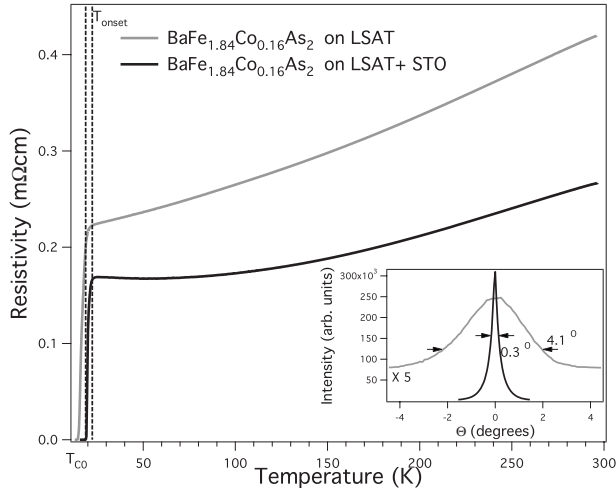


FIG. 1. dc resistivity $\rho(T)$ of $\text{BaFe}_{1.84}\text{Co}_{0.16}\text{As}_2$ film as a function of temperature for films grown on LSAT (gray) and grown with the STO template layer (black). Vertical lines indicate the onset (T_{onset}) and zero resistance temperatures (T_{c0}); T_c is chosen at the middle of this range, 20.6 K with a width of 1.8 K. Inset: x-ray diffraction rocking curve and full width at half maximum for (004) reflection of the films. The intensity for the LSAT film signal is multiplied by 5.

directly on LSAT. For the present film with nominal $x=0.8$, T_c is found to be 20.6 K with a transition width of 1.8 K.

Terahertz conductivity measurements were performed using a home-built terahertz time domain transmission spectrometer (TTDS) at JHU, which in these films can access the frequency range between 200 GHz and 2 THz. In TTDS, a femtosecond laser pulse is split along two paths and excites a pair of photoconductive antennae deposited on radiation damaged silicon on sapphire. A broadband THz pulse is emitted by one antenna, transmitted through the film and measured at the other antenna. By varying the length difference of the two paths, the electric field of the transmitted pulse is mapped out as a function of time. Comparing the Fourier transform of the transmission through the film to that of a reference resolves the full complex transmission coefficient. The transmission is then inverted to obtain the complex conductivity σ by using $t = \frac{n+1}{n+1+Z_0\sigma d}$, where n is the substrate's index and $Z_0=377 \Omega$. By measuring both the magnitude and phase of the transmission, this inversion can be done directly and without Kramers-Kronig transformation. Reference measurements were performed by ratioing to a nominally identical LSAT/STO layered sample. Although explicit effects of the three layers in transmission are possible, additional measurements found the influence of the STO layer to be negligible. The temperature dependence was obtained by placing the sample in a He vapor cryostat with control of the sample temperature between 1.7 and 300 K.

Figure 2 shows the measured THz complex conductivity of $\text{BaFe}_{1.84}\text{Co}_{0.16}\text{As}_2$ for different temperatures. At low temperature the imaginary part exhibits the characteristic $1/\omega$ dependence expected for a superconductor well below T_c . The real part of the conductivity decreases over most of the frequency range as the temperature is lowered below T_c , which is reminiscent of a standard s -wave superconductor.

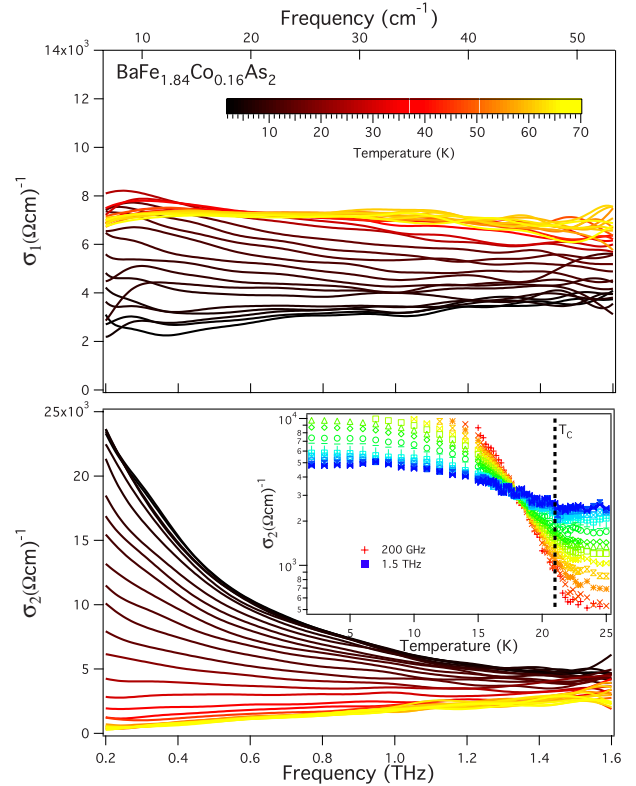


FIG. 2. (Color online) (top) Real part of the THz conductivity of $\text{BaFe}_{1.84}\text{Co}_{0.16}\text{As}_2$. (bottom) Imaginary part of THz conductivity. Inset: temperature dependent σ_2 for several frequencies between 200 GHz (+) and 1.5 THz (■) in 70 GHz steps.

However, at the lowest temperature (2 K), the conductivity is not fully suppressed. As will be discussed below, we interpret this as an indication of pair-breaking effects. Significantly, at low frequencies and slightly below T_c , the real conductivity initially shows a small enhancement before decreasing at low temperature. Enhancement of the dissipative conductivity below T_c has been observed in high-temperature superconductors,²⁰ there the enhancement was discussed in terms of the collapse of the scattering rate in the superconducting state. A signature of this behavior is the shift of the peak in the conductivity to higher temperatures as the probing frequency is increased. We do not observe this shift. We believe our result stems from the coherence peak effect.

In Fig. 3 we show the temperature dependence of the THz conductivity for several frequencies below 2Δ . One can clearly see that just below T_c the conductivity increases above the normal-state value (plots were normalized to the 21 K conductivity). Solid lines in Fig. 3 are fits using the standard Mattis-Bardeen form with a single gap, with $\Delta = 3$ meV, however, fits of similar quality can be obtained using two gaps. Although the theoretical curve qualitatively resembles the data near T_c , at low temperatures the fit is not satisfactory. The theoretical form shows an exponential suppression of the real part of the conductivity at low temperature while the data show a finite residual value of approximately 30%. Although similar residual conductivities have been observed²¹ and interpreted in terms of nodes in the order parameter,^{22,23} as we argue below we believe that the

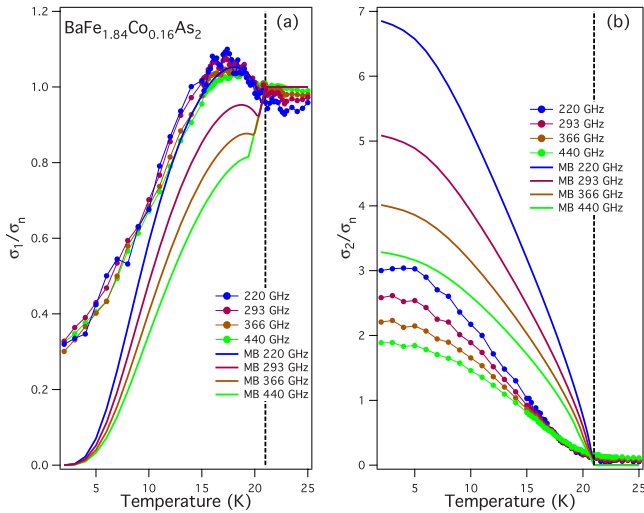


FIG. 3. (Color online) (a) Real and (b) imaginary parts of the THz conductivity as a function of temperature for different frequencies. Solid lines are calculations using the standard Matthis-Bardeen form.

residual conductivity derives from pair-breaking effects.

It is also interesting to note the very narrow temperature region over which superconducting fluctuations are exhibited. As shown in the inset of Fig. 2(b), σ_2 becomes enhanced in region only approximately 2 K above T_c . There is also no sign of an above T_c “dissipation peak” arising from superconducting fluctuations, cf. Fig. 3(a). The narrow range of SC fluctuations may be a reflection of the three-dimensional character of superconductivity in these materials, and are very different from the broad fluctuation range seen via TTDS in the cuprate family of high- T_c superconductors and amorphous thin films.^{24,25}

The observation of the coherence peak in the ac conductivity of $\text{BaFe}_{2-2x}\text{Co}_{2x}\text{As}_2$ is an important clue to the symmetry of the superconducting parameter in this family of materials. A coherence peak is usually taken as evidence of a uniform gap function, although more precisely what is required is that portions of the Brillouin zone coupled by the experimental probe have gaps of the same sign and similar magnitude. Because at terahertz frequencies light’s momentum is at least five orders of magnitude smaller than the reciprocal-lattice momentum, our measurements probe only zero-momentum excitations around the Fermi surface, in the case of the predicted s_{\pm} symmetry in the pnictides superconductors, one expects the conductivity to only detect a single sign of the order parameter since the different sheets are separated by large momentum transfer. Since there is no sign change in the order parameter within a single sheet, we expect a coherence peak that qualitatively resembles that from a single-uniform-gap superconductor.

It is interesting to compare our observation of a coherence peak to the expected one in NMR relaxation rate, i.e., the Hebel-Slichter peak. A number of groups^{26,27} have reported a lack of a coherence peak in the dissipation below T_c . We can interpret these results as follows: as NMR is a local probe that excites a single-species nuclear magnetic resonance, it is sensitive to a superposition over momenta of the nuclear-spin

response, as well as to the momentum-dependent structure factor of the excited nuclei. Thus, NMR relaxation rate is affected by both interband and intraband processes weighted by the appropriate nuclear structure factors. The absence of the coherence peak is natural when gap-sign-changing interband processes dominates the response.^{9,10} It remains to be explained, however, how there could be such a minor contribution to intraband processes.¹⁸

The existence of an s_{\pm} order parameter however is superficially at odds with the residual real conductivity at low temperature. Although such residual conductivity may be consistent with nodes in the order parameter (as they are proposed to exist along the “ c ” axis²²), we feel that overall the data are more consistent with pair-breaking effects and an s_{\pm} order-parameter symmetry. In other cases where nodal excitations have been conclusively identified, like in the d -wave high- T_c superconductors, the intrinsic scattering rates are very small, with the most extreme case being YBCO (<2 GHz).²⁰ That is not the case here, as the width of any low temperature, low-frequency peak is larger than our spectral range (1.8 THz). In contrast, one may expect that pair-breaking effects from impurity scattering are substantial in a superconductor with positive and negative contributions to its order parameter.^{9,10} We expect scattering in these materials because of the effect of Co doping and, in particular, for this films, due to the presence of columnar defects along the c axis.¹⁹

Even more significant evidence for substantial pair breaking comes from the imaginary part of the conductivity [Fig. 3(b)] (which is proportional to the superfluid density) since it is greatly suppressed as compared to the BCS result. In its essence, the Matthis-Bardeen (MB) formalism and its dependence on the size of the superconducting gap is a statement about the conservation of spectral weight in the superconductor. In order to estimate the effects of pair breaking, we calculate the spectral weight missing from the superfluid condensate by subtracting the measured σ_2 from the calculated MB $\sigma_2^{\text{MB}}(T=0)$ as $\hbar\omega[\sigma_2^{\text{MB}}(T=0) - \sigma_2^{\text{measured}}(T=0)]$. If pair breaking is the major contributor to the reduced superfluid density, this difference should be approximately equal to $\frac{\pi}{2}\sigma_1(T=0) \times 2\Delta$ [see Fig. 3(a)]. We find that the residual σ_1 accounts for a substantial 75% of the missing superfluid density from the MB expectation. We expect this estimation to give a lower bound on the effects of pair breaking. We find therefore that observation of a residual σ_1 is consistent with an s_{\pm} pairing symmetry of the gap without nodes. Additional support for our interpretation comes from a comparison with far-infrared conductivity studies of conventional s -wave superconductors doped with magnetic impurities. For an extended s -wave superconductor, nonmagnetic impurities should act the same as magnetic impurities in an s -wave superconductor. The present data bear a strong resemblance to the far-infrared conductivity of Pb films doped with Mn impurities,^{28,29} where a residual value in the zero-frequency limit in σ_1 was found³⁰ but it is in stark contrast with the prediction of Abrikosov *et al.*³¹ where one expects $\sigma_1(\omega \rightarrow 0) = 0$.

The temperature dependence of the penetration depth supports this scenario as well. Figure 4 shows the penetration depth $\lambda(T)$ extracted from the imaginary part of the conduc-

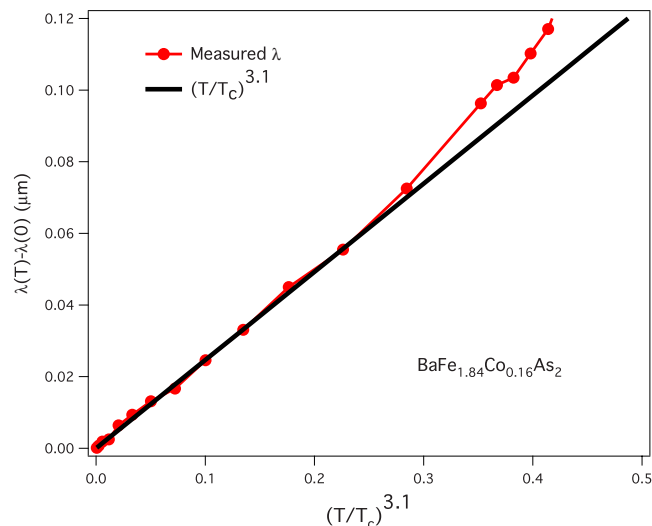


FIG. 4. (Color online) London penetration depth λ of $\text{BaFe}_{1.84}\text{Co}_{0.16}\text{As}_2$ film in a power-law scale as $(T/T_c)^{3.1}$.

tivity at 220 GHz. At low temperature λ follows a power-law behavior with an exponent of 3.1 [Fig. 4(b)]. Although power laws in the penetration depth are typically taken as indicative of the presence of nodes in an order parameter, such a large exponent is generally not consistent with dirty nodal behavior.³² In the present case we think that the large exponents are indicative of pair-breaking excitations. This view is supported by a recent study of the penetration depth measured as a function of Pb radiation-induced disorder³³ in single crystals of $\text{BaFe}_{2-2x}\text{Co}_{2x}\text{As}_2$. The authors found that the exponent decreased with increasing disorder and that cleaner samples have a larger exponent and was consistent with pair-breaking effects. Based on a model of $s\pm$ symmetry of the gap without nodes, they were able to explain the

trend with disorder. Although our large exponent power law of more than three is in contrast to microwave and far-infrared measurements in single crystals³⁴ and thin films,²³ where a smaller exponent closer to 2 has been observed, it is consistent with the excellent quality of our films. In addition, calculations^{35,36} of the microwave conductivity and penetration depth that take into account the pair-breaking scattering due to impurities in a multiband $s\pm$ superconductor, reproduce both our observations of finite absorption below the gap [cf. Fig. 3(a)] and a power-law dependence of the penetration depth (cf. Fig. 4) at low temperatures. This calculation places the impurity scattering in $\text{BaFe}_{2-2x}\text{Co}_{2x}\text{As}_2$ between the Born and unitary limits. Similar observation has been made in single crystals of $\text{BaFe}_{2-2x}\text{Co}_{2x}\text{As}_2$.³⁷

We have reported evidence that support the extended s -wave scenario for the symmetry of the superconducting gap in $\text{BaFe}_{1.84}\text{Co}_{0.16}\text{As}_2$. In particular, the presence of the coherence peak in the THz conductivity, the power-law behavior of the penetration depth λ with a high exponent, and presence of pair-breaking scattering are consistent with an $s\pm$ symmetry of the order parameter which does not contain nodes. We hope that our work stimulates further investigation into the effects of pair breaking in these compounds. In particular, detailed calculations of their effects on the conductivity in the superconducting state would be very useful.

This work was supported under the auspices of the Institute for Quantum Matter, DOE under Grant No. DE-FG02-08ER46544 at JHU. Work at UW was supported by DOE Office of Basic Energy Sciences under Award No. DE-FG02-06ER46327 and work at NHMFL supported by NSF under Grant No. DMR-0084173, by the State of Florida, and by AFOSR under Grant No. FA9550-06-1-0474. We would like to thank A. Bernevig, G. Boyd, R. Gordon, K. Moler, J. Murray, V. Stanev, Z. Tešanović, and D. Wu for useful discussions.

*rvaldes@pha.jhu.edu

†npa@pha.jhu.edu

¹Y. Kamihara *et al.*, *J. Am. Chem. Soc.* **130**, 3296 (2008).

²M. Rotter *et al.*, *Phys. Rev. Lett.* **101**, 107006 (2008).

³F.-C. Hsu *et al.*, *Proc. Natl. Acad. Sci. U.S.A.* **105**, 14262 (2008).

⁴X. Wang *et al.*, *Solid State Commun.* **148**, 538 (2008).

⁵A. S. Sefat *et al.*, *Phys. Rev. Lett.* **101**, 117004 (2008).

⁶J.-H. Chu *et al.*, *Science* **329**, 824 (2010).

⁷M. A. Tanatar *et al.*, *Phys. Rev. B* **81**, 184508 (2010).

⁸V. Cvetkovic *et al.*, *EPL* **85**, 37002 (2009).

⁹I. I. Mazin *et al.*, *Phys. Rev. Lett.* **101**, 057003 (2008).

¹⁰A. V. Chubukov *et al.*, *Phys. Rev. B* **78**, 134512 (2008).

¹¹J. Bardeen *et al.*, *Phys. Rev.* **108**, 1175 (1957).

¹²D. C. Mattis *et al.*, *Phys. Rev.* **111**, 412 (1958).

¹³M. Tinkham, *Introduction to Superconductivity* (Dover, New York, 2004), Chap. 3.

¹⁴L. C. Hebel *et al.*, *Phys. Rev.* **113**, 1504 (1959).

¹⁵L. H. Palmer *et al.*, *Phys. Rev.* **165**, 588 (1968).

¹⁶K. Matano *et al.*, *EPL* **83**, 57001 (2008).

¹⁷Y. Nakai *et al.*, *J. Phys. Soc. Jpn.* **77**, 073701 (2008).

¹⁸M. M. Parish *et al.*, *Phys. Rev. B* **78**, 144514 (2008).

¹⁹S. Lee *et al.*, *Nature Mater.* **9**, 397 (2010).

²⁰A. Hosseini *et al.*, *Phys. Rev. B* **60**, 1349 (1999).

²¹B. Gorshunov *et al.*, *Phys. Rev. B* **81**, 060509 (2010).

²²J.-P. Reid *et al.*, *Phys. Rev. B* **82**, 064501 (2010).

²³T. Fischer *et al.*, arXiv:1005.0692 (unpublished).

²⁴J. Corson *et al.*, *Nature (London)* **398**, 221 (1999).

²⁵R. W. Crane *et al.*, *Phys. Rev. B* **75**, 094506 (2007).

²⁶K. Ahilan *et al.*, *Phys. Rev. B* **78**, 100501 (2008).

²⁷F. Ning *et al.*, *J. Phys. Soc. Jpn.* **77**, 103705 (2008).

²⁸G. Dick *et al.*, *Phys. Rev.* **181**, 774 (1969).

²⁹M. Woolf *et al.*, *Phys. Rev.* **137**, A557 (1965).

³⁰It was also found (Refs. 28 and 29) that Pb films with Gd impurities did follow the expected behavior based on the Abrikosov-Gorkov theory (Ref. 31).

³¹A. A. Abrikosov *et al.*, *Sov. Phys. JETP* **12**, 1243 (1961).

³²P. J. Hirschfeld and N. Goldenfeld, *Phys. Rev. B* **48**, 4219 (1993).

³³H. Kim *et al.*, *Phys. Rev. B* **82**, 060518 (2010).

³⁴R. T. Gordon *et al.*, *Phys. Rev. Lett.* **102**, 127004 (2009).

³⁵O. V. Dolgov *et al.*, *New J. Phys.* **11**, 075012 (2009).

³⁶A. B. Vorontsov *et al.*, *Phys. Rev. B* **79**, 140507 (2009).

³⁷R. P. S. M. Lobo *et al.*, *Phys. Rev. B* **82**, 100506 (2010).